buildings

MDPI

Article

Effect of Steel Support Cross-Section and Preloaded Axial Force on the Stability of Deep Foundation Pits

Yang Jin [1], Hanzhe Zhao [2], Chuanfeng Zheng [2,*], Jian Liu [1] and Chong Ding [1]

[1] Communications Construction Company of CSCEC 7th Division Co., Ltd., Zhengzhou 450004, China; 18638486064@163.com (Y.J.)
[2] College of Transportation, Jilin University, Changchun 130012, China; zhaohz22@mails.jlu.edu.cn
* Correspondence: cfzheng@jlu.edu.cn

Abstract: To investigate the effects of steel support cross-section dimensions and preloaded axial force levels on the stability of foundation pits, numerical simulations were conducted for open-cut deep foundation pits based on monitoring data from Changchun Metro Line 9. Results show that increasing the wall thickness and diameter of the steel support significantly reduces the horizontal displacement and axial force of the enclosure pile. When the wall thickness increases from 14 mm to 25 mm, the horizontal displacement of the enclosure pile can be reduced by up to 7.63 mm, and the axial force of the steel support can be reduced by 11.4–15%. When the diameter of the steel support changes from 609 mm to 800 mm, the axial force of the second steel support is reduced by 3.2–5.5%. The change in preloaded axial force results in a horizontal displacement change of about 3–5 mm and a surface settlement change of about 0.6–4.2 mm. The preloaded axial force meets pit stability control requirements when it reaches 60% of the design axial force.

Keywords: deep subway foundation pit; steel support; cross-section dimensions; preloaded axial force; numerical simulation; stability analysis

Citation: Jin, Y.; Zhao, H.; Zheng, C.; Liu, J.; Ding, C. Effect of Steel Support Cross-Section and Preloaded Axial Force on the Stability of Deep Foundation Pits. *Buildings* **2024**, *14*, 2532. https://doi.org/10.3390/buildings14082532

Academic Editor: Mizan Ahmed

Received: 9 July 2024
Revised: 1 August 2024
Accepted: 5 August 2024
Published: 16 August 2024

1. Introduction

With the rapid development of urban construction in recent years, the construction of urban subways has increased to facilitate the travel of the public and ease traffic pressure. The construction of a deep foundation pit is an important link in the process of subway construction, and the ensuing problem of deep foundation pit safety has attracted much attention. As an important part of the deep foundation pit support structure, the internal support should be given full attention in the design and construction process. In existing projects, steel supports are widely used due to their advantages of high strength, strong load bearing capacity, short construction period, and reusability [1–3]. However, because of the unreasonable design of cross-section dimensions and insufficient preloaded axial force, a risk of instability in deep foundation pits supported by steel remains. Therefore, fully exploring the effect of steel supports on the stability of deep foundation pits is important for the safe construction of future subway projects.

The cross-section size and preloaded axial force level of steel supports are important considerations in the design of deep foundation pits. Different cross-section sizes and preloaded axial force levels have a great impact on the horizontal displacement and axial force of the enclosure structure [4–8], which is why their potential risks should not be ignored. If the horizontal displacement of the enclosure structure is too large, then the deep foundation pit will be prone to the risk of destabilising and damaging the enclosure structure and to the risk of the pit bottom bulging [9–14]. If the axial force of the steel support exceeds the design value, then the risk of destabilising and damaging the internal support is prone to occur [15–18]. Most scholars analyse the stability of the deep foundation pit from the change in water level inside and outside the pit, the stability of the enclosing

structure, and the adverse geological conditions, but the influence of the steel support on the stability of the deep foundation pit should not be ignored [19–22]. The deformation law of steel supports has been emphasised by many scholars, but the variation in detail size and preloaded axial force is still what should be focused on. Therefore, the cross-section size and preloaded axial force level of the steel support need to be designed scientifically to minimise the probability of risk occurrence and thus ensure the stability of the deep foundation pit, thereby reducing the construction cost and rationally utilising the underground space of cities.

In this paper, based on our previous work, we investigate the effect of parameters such as fine dimensions (diameter and wall thickness) and preloaded axial force of steel supports on the stability of deep foundation pits. ABAQUS software (v. 2020HF5) is used to numerically simulate the foundation pit structure and excavation process of Changchun Metro Line 9 (Airport Line), and the accuracy of the numerical model is verified by using on-site monitoring data to analyse the effects of the cross-section size of the steel support and the pre-added axial force on the horizontal displacement of the pile, the axial force of the steel support, and the settlement of the ground surface. The research flowchart is shown in Figure 1.

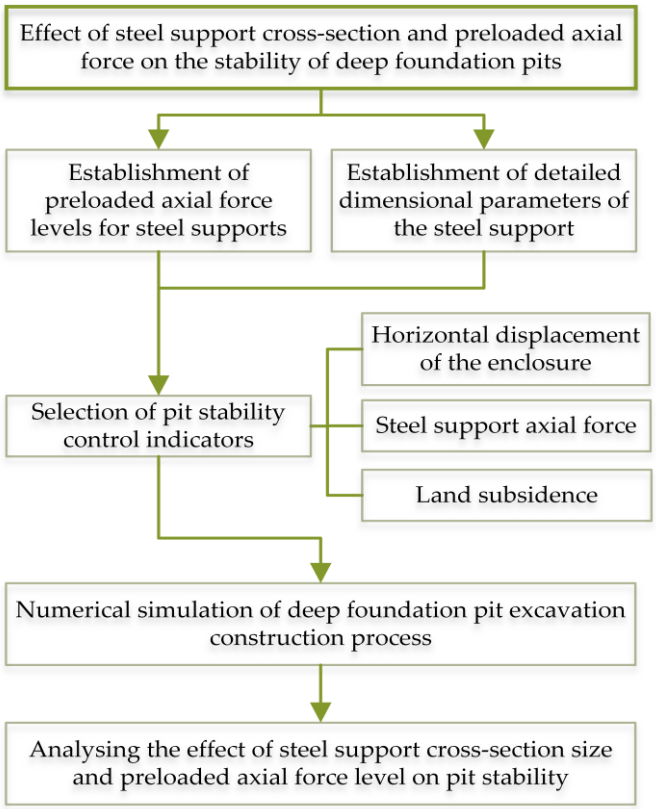

Figure 1. Flowchart of the research route.

2. Project Overview

This project focuses on the Changchun City Urban Railway Airport Line Section II Cut-and-cover Deep Foundation Pit Project in Jilin Province, China. The total length of the open-cut interval pit is 629.97 m, of which the length of the rectangular frame is 422.98 m, the length of the U-type groove section is 205.9 m, the width of the foundation pit is 15.5–21.1 m, and the depth of excavation of the foundation pit is 0–13.1 m. The location of the deep foundation pit is shown in the layout plan in Figure 2.

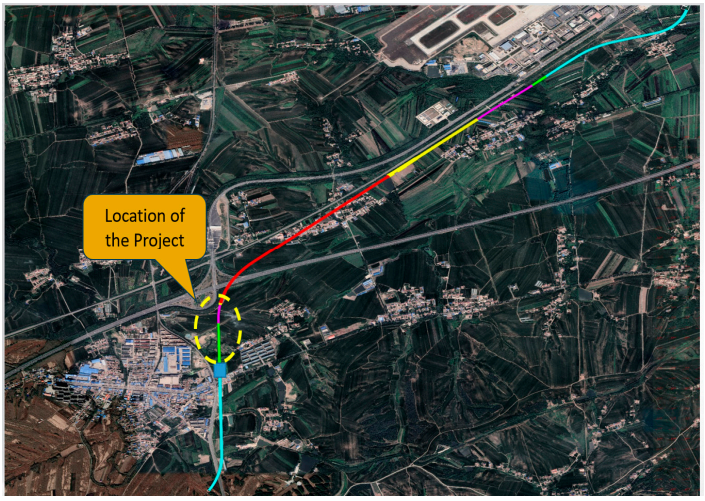

Figure 2. Plan view of deep foundation pit.

The support structure of the excavated pit has a multi-pivot pile support system plus an external precipitation programme. The open excavation foundation pit enclosure structure adopts two kinds of bored pile structure, one with a pile diameter of 800 mm and pile spacing of 1300 mm, and the other with a pile diameter of 600 mm and pile spacing of 1000 mm. The crown beam has a reinforced concrete structure, of which the cross-section size of the φ600 bored pile range is 600 mm × 1000 mm, the rest of the cross-section size is 800 mm × 1000 mm, and the crown beam is C30 concrete. In the foundation pit, two supports (local two) + one replacement support (local) are used. The steel support specifications are φ609 mm (t = 16 mm) and φ800 mm (t = 16 mm). The first steel support is propped on the crown girder, and the rest of the steel supports are propped on drilled piles through the double splicing work 40b horizontal steel purlins, as shown in Figure 3.

Figure 3. Arrangement of steel supports.

3. Numerical Simulation of Deep Foundation Pit

3.1. Geometric Modelling

The deep foundation pit of the subway in this project adopts the support structure of drilled piles + steel support. On the basis of current research experience, when the finite element numerical model is being constructed, the enclosure in the form of drilled piles can be simplified to a diaphragm wall according to the principle of equivalent stiffness [23].

The pile diameter of the bored piles in the project is D = 800 mm, and the pile spacing t = 1300 mm. The thickness of the diaphragm wall after the equivalent calculation according to Equations (1) and (2) is h = 0.486 m. After simplification, the model is built with three-dimensional solid units, and the depths of the enclosing piles are 11.2, 15.5, and 10.5 m.

$$\frac{(D+t)h^3}{12} = \frac{\pi D^4}{64} \tag{1}$$

$$h = \sqrt[3]{\frac{3\pi D^4}{16(D+t)}} \tag{2}$$

where D is the diameter of bored piles, t is the spacing of bored piles, and h is the thickness of the diaphragm wall.

The parts include the diaphragm wall enclosure, steel support, and soil model, where the steel support is modelled in the form of a beam unit, and the rest are modelled as three-bit solid units.

The dimensions after assembling the components with the excavation construction schematic are shown in Figure 4.

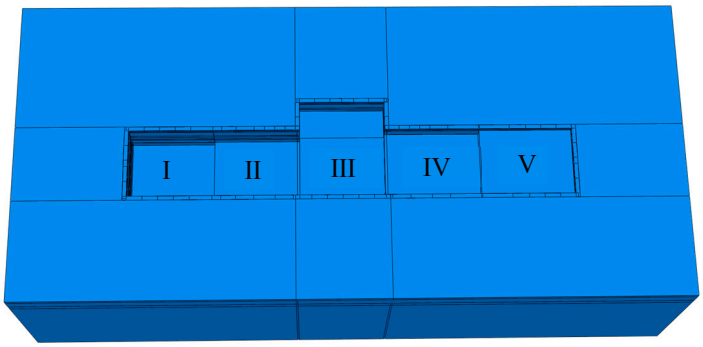

Figure 4. Geometric model of deep foundation pit; overall schematic diagram of excavation construction.

3.2. Selection of Material Parameters

Based on the provided *Changchun City Urban Rail Transit Line Phase I Project Donghuan Road Station~Phase I Terminal Interval Rockstone Engineering Detailed Lecha* and the *Chinese Geological Engineering Handbook* [24], the engineering geological profile of the project is added below. The parameters of the soil layer are shown in Table 1. The Mohr–Coulomb constitutive model was chosen to describe the stress–strain relationship of the soil in the numerical model in this paper. The model is widely used to describe the plastic behaviour of soils and provides a simple and effective damage criterion to predict the damage conditions of materials under different stress states, which helps in engineering design and stability analysis.

Table 1. Soil layer parameters of Changchun Metro Line 9 deep foundation pit project.

Soil Layer	Density/(kg/m^3)	Internal Friction Angle/°	Cohesive Force/kPa	Poisson's Ratio	Elastic Modulus/MPa
Silty Clay	2000	20	33	0.25	39
Mudstone	2500	25	50	0.25	6000
Conglomerate	2140	28	40	0.25	11,000

The soil body is divided into three layers. The first layer of the soil body is powdery clay with a depth of 3.709 m, the second layer is mudstone with a depth of 1.6 m, and the third layer is conglomerate with a depth up to the bottom of the soil body model, as shown in Figure 5. The material of the bored piles of the enclosure structure is C30 concrete, and the material of the steel support is Q235B steel; the specific parameters are shown in Table 2.

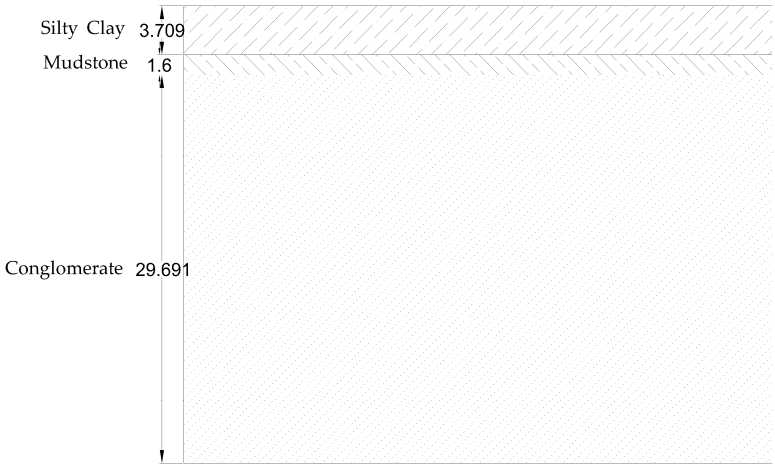

Figure 5. Schematic distribution of soil layers.

Table 2. Material parameters of deep foundation pit support structure of Changchun Metro Line 9.

Materials	Density/(kg/m^3)	Elastic Modulus/MPa	Poisson's Ratio
C30 Concrete	2450	30,000	0.3
Q235B Steel	7850	210,000	0.3

3.3. Analysis Step Establishment

In this process, the deep foundation pit is divided into five vertical segments and vertically divided into five layers of step excavation, with excavation being performed on the position of the steel support erection of the following 0.5 m, at which point digging is stopped. The maximum depth of each layer of excavation does not exceed 2 m. The step design was analysed according to the deep foundation pit construction sequence, as shown in Table 3.

Table 3. Numerical simulation analysis step design for deep foundation pit.

Step	Analysis Step Content	Step	Analysis Step Content
1	Ground Stress Equilibrium	10	Erection of The Second Steel Support for Section II and The First Steel Support for Section IV.
2	Enclosure Construction	11	I Section V, II Section IV, III Section III, IV Section II, V Section I Soil Excavation
3	Excavation of The First Layer of Soil in Section I	12	Erection of The Second Steel Support for Section III and The First Steel Support for Section V.
4	Erection of The First Steel Support for Section I	13	II Section V, III Section IV, IV Section III, V Section II Soil Excavation
5	Excavation of The Second Layer of Section I and The First Layer of Section II	14	Erection of The Second Steel Support for Section IV
6	Erection of The First Steel Support for Section II	15	Excavation of The Soil in Layer 5 of Section III, Layer 4 of Section IV, Layer 3 of Section V
7	Excavation of Soil in Layer 3 of Section I, Layer 2 of Section II, Layer 1 of Section III	16	Excavation of Soil in Layer 5 of Section IV and Layer 4 of Section V
8	Erection of The First Steel Support for Section III	17	Excavation of Soil Layer 5 of Section V
9	Excavation of Soil in Layer 4 of Section I, Layer 3 of Section II, Layer 2 of Section III, Layer 1 of Section IV		

3.4. Contact and Boundary Condition Settings

The contact between the diaphragm wall and the soil body is surface-to-surface contact, with normal behaviour of the hard contact, tangential behaviour of the penalty, and a friction coefficient of 0.2; the contact between the steel support and the diaphragm

wall has a bound constraint; and the contact between the steel purlin and the diaphragm wall has a built-in constraint.

The boundary conditions of the numerical model are set as follows: the boundary surfaces on both sides in the X direction constrain the X-direction displacement; the boundary surfaces on both sides in the Y direction constrain the Y-direction displacement; and the bottom surface in the Z direction constrains the X-direction, Y-direction, and Z-direction displacements. The setting of the model boundary is shown in Figure 6.

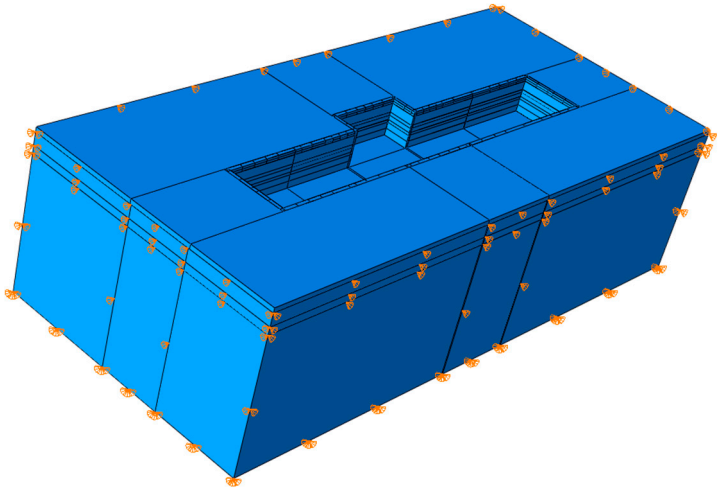

Figure 6. Schematic diagram of model boundary conditions.

3.5. Meshing

In this study, the 3D solid cell C3D8R is used for the enclosure structure and soil body model, and the B31 beam cell form is used for the steel support and steel purlin. The grid size of the soil cell varies from 1 m to 3 m, the grid size of the enclosure structure cell is 1 m, and the grid size of the steel support and steel purlin cell is 0.5 m, which ensures the computational accuracy of the critical areas. The complex geometric regions were automatically refined by the adaptive mesh technology of ABAQUS. The quality of the delineated grid was checked, and the distortion, aspect ratio, and other indexes of all cells were within reasonable range, ensuring the quality of the grid and the stability of the calculation.

3.6. Numerical Model Validation

The arrangement of monitoring points relying on the physical works of the project is shown in Figure 7. ZDS stands for horizontal displacement of the pile top, ZDC stands for vertical displacement of the pile top, DB stands for surface settlement, ZT stands for pile displacement, and ZL stands for shaft force. The results of surface settlement calculated by ABAQUS software are shown in Figure 8. According to the numerical simulation results, there is a maximum value of 6.2 mm of surface settlement at the location of pile DB-72-01, which is a reduction of 1.6 mm compared with the monitoring value. The horizontal displacement and surface settlement in the measured values are selected and compared with the numerical simulation results, as shown in Figure 9. The overall trend in the measured and simulated values of horizontal displacement and surface settlement at the top of the pile is basically the same, and the difference is about 0.2–2.6 mm, which shows that the accuracy of the numerical model can meet the needs of engineering calculation and analysis.

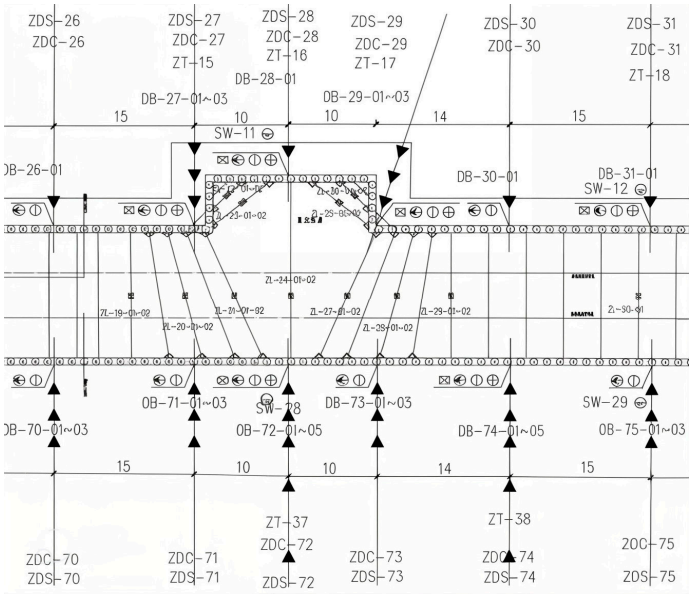

Figure 7. Layout of monitoring sites.

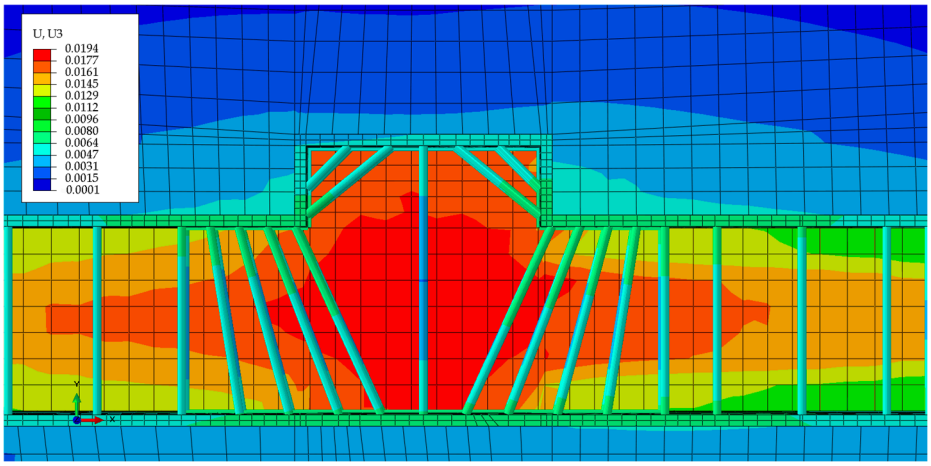

Figure 8. Deep foundation pit surface settlement cloud map.

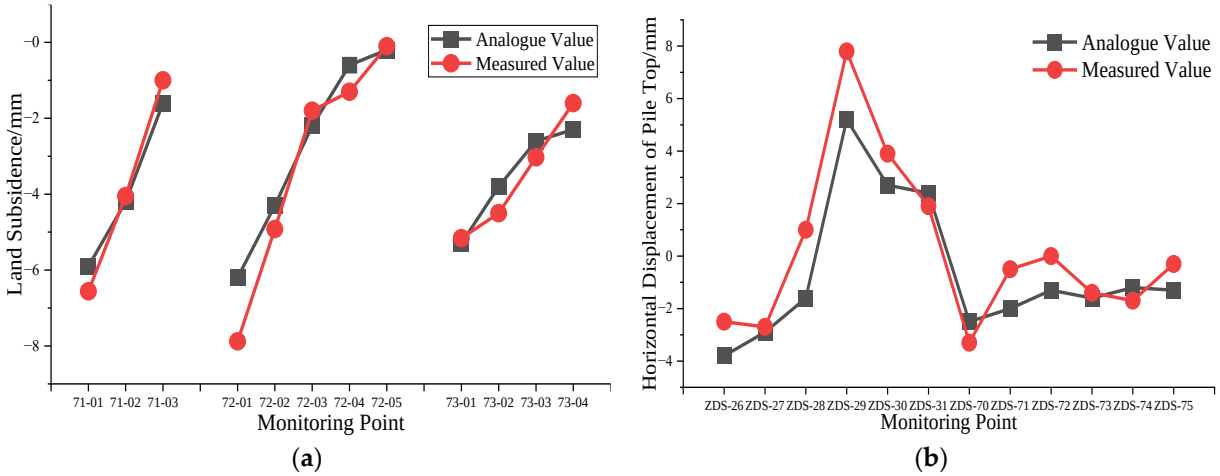

Figure 9. Comparison of measured and simulated values. (**a**) Comparison of measured and simulated surface settlements; (**b**) comparison of measured and simulated horizontal displacement of pile tops.

4. Mechanical Response Analysis of Steel Support in Deep Foundation Pit

4.1. Establishment of Evaluation Indicators

On the basis of the calculation results of numerical simulation, the change in the steel support cross-section size and preloaded axial force does not have a significant effect on the effect of pit bottom bulge rebound and pile vertical displacement. Therefore, the horizontal displacement of the enclosure structure, the axial force of the steel support, and the surface settlement were selected as the evaluation indexes of the stability of the deep foundation pit. The deep foundation pit monitoring level of the Changchun Metro Line 9 subway second working area is on the second level, and the monitoring index control value interval was determined according to the specifications of the Technical standard for monitoring measurement of urban rail transit engineering [25], as shown in Table 4.

Table 4. Monitoring control values for open-cut support structures and surrounding geotechnical bodies.

Monitoring Projects	Engineering Monitoring Level II		
	Cumulative Value/mm		Rate of Change/(mm/d)
	Absolute Value	Relative Pit Depth (H) Value	
Vertical Displacement of Pile Top	20–30	0.15–0.3%	3–4
Horizontal Displacement of Pile Top	20–30	0.15–0.3%	3–4
Horizontal Displacement of Pile Body	30–40	0.2–0.4%	3–4
Surface Settlement	25–35	0.2–0.3%	2–4
Rebounding of Pit Bottom Elevation	25–35		2–3
Supporting Axial Force		Maximum Value: (70–80%) f Minimum Value: (80–100%) f_y	

Note: The support axial force is controlled within the range of 80–100% of the design value of prestressing for supports and anchors as a minimum value and 80–100% of the design value of the load-bearing capacity of members.

The depth of the foundation pit in this project is H = 8.245 m. Thus, the control value of horizontal displacement and vertical displacement of the pile top is 12.37–24.74 mm, that of the horizontal displacement of the pile body is 16.49–32.98 mm, and that of surface settlement is 16.49–24.74 mm. The preloaded axial force of the first steel support is 212–950 kN, and the control value of the first steel support is 169–950 kN. The preloaded axial force of the second steel support is 975.2–4370 kN, and the control value is 780.16–4370 kN.

4.2. Effect of Steel Support Cross-Section Size on Pit Stability

For the study of the effect of steel support cross-section size on the axial force and horizontal displacement of the enclosure structure, the diameter of the steel support was selected as 609 and 800 mm, and the wall thickness of the pipe was selected as 12, 14, 16, 18, 20, and 25 mm, totalling 12 cross-section sizes of the steel support.

4.2.1. Effect of Cross-Section Dimensions on Horizontal Displacements of Enclosures

The change rule of horizontal displacement with the depth of the enclosure structure under different cross-section sizes was obtained through finite element simulation, which is shown in Tables 5 and 6. Table 5 presents the calculation results of the steel support with a diameter of 609 mm, and Table 6 presents the calculation results of the steel support with a diameter of 800 mm.

The horizontal displacement versus depth curves of the pit enclosure structure for different steel support cross-section characteristic conditions are shown in Figure 10.

Table 5. Horizontal displacement change rule of enclosure structure with depths under different wall thickness conditions.

Depths/m	Diameter 609 mm Steel Support Wall Thickness/mm					
	12 mm	**14 mm**	**16 mm**	**18 mm**	**20 mm**	**25 mm**
0	9.27	8.03	7.09	6.55	5.73	4.64
0.50	7.93	6.94	6.17	5.76	5.08	4.20
1.00	6.60	5.84	5.26	4.96	4.42	3.75
1.13	6.23	5.51	4.96	4.68	4.18	3.55
2.00	3.88	3.43	3.09	2.92	2.60	2.22
3.00	6.18	5.26	4.56	4.13	3.55	2.75
3.85	9.43	8.03	6.94	6.29	5.39	4.16
4.70	1.49	1.20	0.98	0.84	0.68	0.44
5.70	−7.04	−6.14	−5.44	−4.54	−3.97	−2.87
6.70	−11.67	−10.21	−9.06	−7.58	−6.65	−4.83
7.47	−13.46	−11.83	−10.55	−8.85	−7.80	−5.72
8.24	−14.57	−12.86	−11.51	−9.70	−8.58	−6.34
9.20	−15.46	−13.71	−12.33	−10.43	−9.26	−6.90
10.15	−15.91	−14.17	−12.78	−10.85	−9.66	−7.24
11.11	−16.08	−14.36	−12.99	−11.06	−9.87	−7.44
12.07	−15.90	−14.24	−12.92	−11.02	−9.85	−7.46
12.95	−15.25	−13.69	−12.44	−10.63	−9.52	−7.23
13.84	−13.69	−12.31	−11.21	−9.59	−8.60	−6.54
14.73	−10.67	−9.60	−8.75	−7.49	−6.72	−5.12
15.62	−6.65	−5.99	−5.46	−4.67	−4.19	−3.20
16.50	−5.42	−4.88	−4.44	−3.80	−3.41	−2.59

Table 6. Horizontal displacement change rule of enclosure structure with depths under different wall thickness conditions.

Depths/m	Diameter 800 mm Steel Support Wall Thickness/mm					
	12 mm	**14 mm**	**16 mm**	**18 mm**	**20 mm**	**25 mm**
0	8.57	7.42	6.38	5.42	4.52	3.54
0.50	7.52	6.59	5.73	4.91	4.14	3.32
1.00	6.47	5.75	5.06	4.40	3.75	3.09
1.13	6.12	5.44	4.79	4.16	3.55	2.92
2.00	3.85	3.42	3.01	2.62	2.23	1.84
3.00	5.60	4.73	3.97	3.29	2.68	1.99
3.85	8.51	7.18	6.01	4.97	4.04	2.99
4.702	1.22	0.95	0.73	0.56	0.41	0.24
5.70	−6.66	−5.79	−4.98	−3.81	−3.19	−2.23
6.70	−11.10	−9.68	−8.37	−6.42	−5.38	−3.80
7.47	−12.91	−11.32	−9.84	−7.59	−6.38	−4.55
8.24	−14.09	−12.42	−10.83	−8.39	−7.09	−5.09
9.20	−15.08	−13.36	−11.72	−9.12	−7.73	−5.60
10.15	−15.63	−13.91	−12.25	−9.56	−8.14	−5.94
11.11	−15.88	−14.18	−12.53	−9.81	−8.37	−6.13
12.07	−15.78	−14.13	−12.51	−9.82	−8.39	−6.18
12.95	−15.18	−13.63	−12.09	−9.50	−8.13	−6.00
13.84	−13.67	−12.29	−10.91	−8.59	−7.36	−5.44
14.73	−10.67	−9.60	−8.54	−6.72	−5.76	−4.27
15.62	−6.65	−5.99	−5.32	−4.19	−3.59	−2.66
16.50	−5.42	−4.87	−4.32	−3.40	−2.91	−2.15

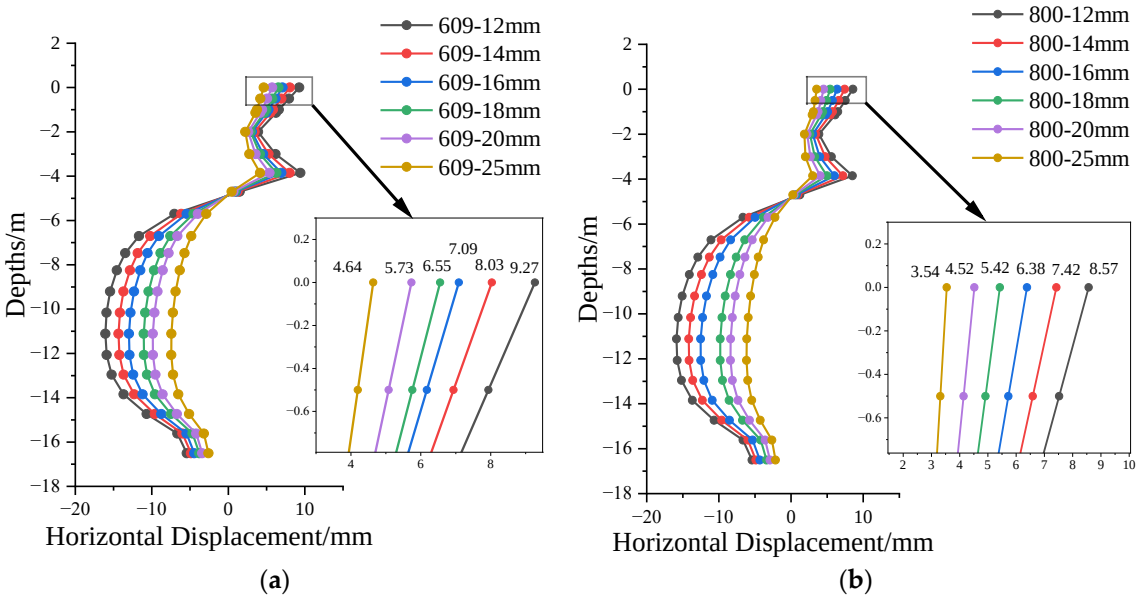

Figure 10. Horizontal displacement change rule of pit enclosure structure with depths under different conditions of steel support cross-section characteristics. (**a**) The diameter of the steel support is 609 mm; (**b**) the diameter of the steel support is 800 mm.

Figure 10 shows that the change in the cross-section size of the steel support has a large influence on the horizontal displacement of the enclosure structure. When the diameter of the steel support is 609 mm, the horizontal displacement of the pile top with a 12 mm wall thickness is 9.27 mm, which is 99.8% higher than that of the pile top with a 25 mm wall thickness. When the wall thickness of the steel support is 25 mm, the horizontal displacement of the pile top with an 800 mm diameter is 3.54 mm, which is 23.7% lower than that of the steel support with a 609 mm diameter. Increasing the wall thickness and diameter of the steel support can significantly increase the stiffness of the support and reduce the deformation of the enclosure. After further data analysis, the horizontal displacement of the pile top with a 609 mm steel support diameter and a 25 mm wall thickness is close to the value with an 800 mm diameter and a 20 mm wall thickness. In addition, the horizontal displacement of the pile top with a 609 mm steel support diameter and a 20 mm wall thickness is close to the value with an 800 mm diameter and an 18 mm wall thickness. This suggests that within a certain range of coupled effects of steel support diameter and wall thickness on pit safety, variations in diameter and wall thickness can compensate for each other to achieve a similar effect.

4.2.2. Effect of Steel Support Cross-Section Size on Axial Force

Three internal supports were taken from the numerical model of the deep foundation pit for axial force analysis, which are the first internal support of Section II, the first internal support of Section III, and the second internal support of Section III. Their steel support axial force variation curves with the analysis of step time are shown in Figure 11.

As can be seen from Figure 11, when the diameter of the control steel support is constant, increasing the wall thickness decreases the axial force. When the wall thickness of the control pipe is constant, increasing the diameter decreases the axial force. When the control diameter is the same, the change in the axial force of the second steel support is significantly higher than that of the first steel support, and when the diameter is 609 mm, the axial force of the second steel support with a wall thickness of 12 mm increases by 68.2% compared with that with a wall thickness of 25 mm. The increase in the thickness and diameter of the steel support improves the overall stiffness of the support, which makes the stress distribution under the external force more uniform and reduces the local deformation and stress concentration. In the structural design, the axial force can be

reduced by appropriately increasing the wall thickness or diameter of the steel support to improve the safety and stability of the support system.

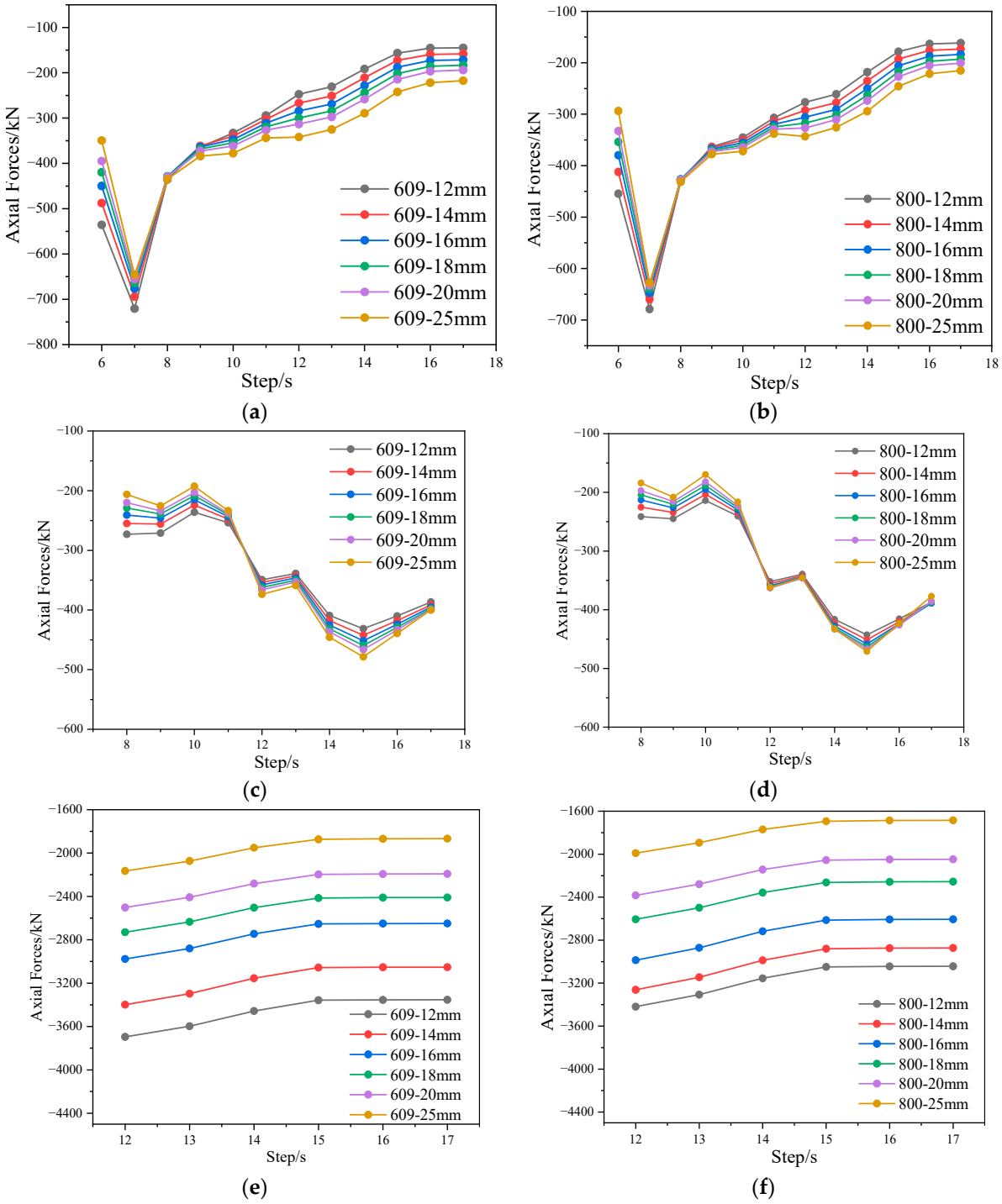

Figure 11. The change rule of axial stress of steel supports with time under the condition of different cross-section sizes. (**a**) Section II: 609 mm diameter first steel support axial force change rule with time; (**b**) Section II: 800 mm diameter first steel support axial force change rule with time; (**c**) the change rule of axial force with time for the first steel support with a 609 mm diameter in Section III; (**d**) the pattern of change in the axial force with time for the first steel support with an 800 mm diameter in Section III; (**e**) the pattern of change in the axial force with time for the second steel support with a 609 mm diameter in Section III; (**f**) the pattern of change in the axial force with time for the second steel support with an 800 mm diameter in Section III.

4.3. Effect of Preloaded Axial Force of Steel Support on the Stability of the Deep Foundation Pit

The horizontal displacement and surface settlement of the enclosure structure were selected as the control indexes, and 60%, 70%, 80%, 90%, 100%, 110%, and 120% of the designed axial force were selected as the preloaded axial force levels to study the effect of preloaded axial force of steel support on the safety of the deep foundation pit.

4.3.1. Effect of Preloaded Axial Force of Steel Support on Horizontal Displacement of Enclosure Structure

The variation rule of horizontal displacement of the enclosure with depths under different preloaded axial forces is shown in Figure 12.

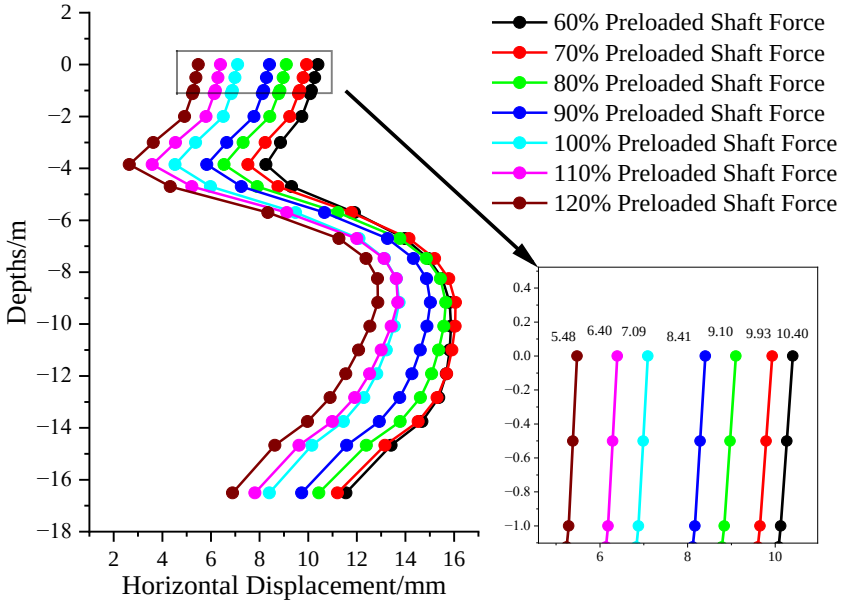

Figure 12. Horizontal displacement change rule of enclosure structure with depths under different preloaded axial force conditions.

This figure shows that the preloaded axial force affects the horizontal displacement of the pile top, which is 5.48 mm when the preloaded axial force level is 120% and 10.40 mm when the preloaded axial force level is 60%. Further analysis shows that even if the preloaded axial force level is 60%, the value of horizontal displacement of the pile top is within the permissible range. Thus, reducing the preloading level appropriately is feasible under the premise of satisfying the safety of the foundation pit.

4.3.2. Effect of Steel Support Preloaded Axial Force on Surface Settlement

For the analysis of the effect of steel support preloaded axial force on the surface settlement, a horizontal path was set in the middle of the deep foundation pit to analyse the change in surface settlement with the horizontal route under different preloaded axial forces, and the curves are plotted in Figure 13.

As can be seen from Figure 13, a large horizontal distance from the pit corresponds to small surface settlement. When the horizontal distance reaches 20 m, the surface settlement is close to 0, which reflects the general law of the pit surface settlement. The size of the preloaded axial force is correlated with the surface settlement; a larger preloaded axial force will produce smaller surface settlement, and when the preloaded axial force decreases, the surface settlement will increase. For example, at a preloaded axial force level of 120%, the surface settlement is 6.3 mm. At a preloaded axial force level of 60%, the surface settlement is 10.5 mm. Increasing the preloaded axial force improves the stiffness and bearing capacity of the support system, which is able to resist earth pressure and reduce soil displacement and settlement around the pit.

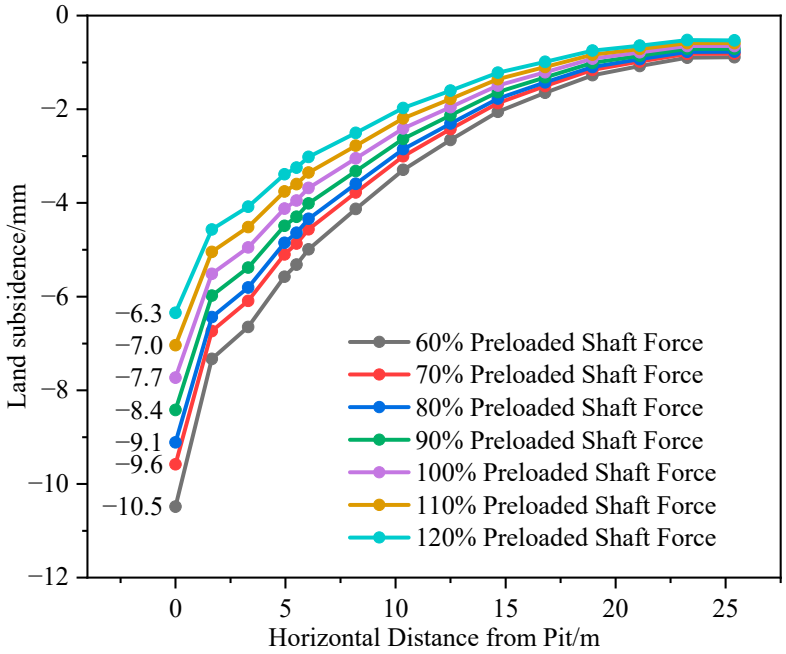

Figure 13. Foundation surface settlement under different preloaded axial force conditions.

5. Discussion

Based on the findings in this paper, the following recommendations are made for similar foundation pit projects:

(1) The diameter and wall thickness of the steel support have a significant effect on both the horizontal displacement and axial force of the enclosure structure. Space constraints and material costs need to be considered comprehensively in the design.
(2) During the excavation and support of the foundation pit, a real-time monitoring system should be set up to monitor key parameters such as surface settlement and axial force of steel support.
(3) During the design and construction process, it is also necessary to comprehensively consider the influence of factors such as the nature of the soil, changes in the water table, and the construction process on the surface settlement. Through multi-factor analysis, a more comprehensive and scientific foundation pit support programme can be developed.

6. Conclusions

The following conclusions were obtained by analysing the effect of changes in steel support cross-section size and preloaded axial force on the horizontal displacement of deep foundation pit enclosure structures, steel support axial force, and surface settlement:

(1) As an important part of the deep foundation pit structure, the detailed characteristics of the steel support will affect the safety of the foundation pit, and quantitative evaluation of the effect of the steel support diameter, wall thickness, and preloaded axial force level on the safety of the foundation pit has considerable engineering significance.
(2) Under the same diameter, the horizontal displacement of the enclosing pile changes from 4.64 mm to 13.55 mm as the wall thickness increases from 14 mm to 25 mm, and the axial force of the second steel support decreases by 11.4% to 15% for every 2 mm increase in wall thickness.
(3) When the diameter of the steel support changes from 609 mm to 800 mm, the axial force of the second steel support decreases by 3.2–5.5%. The analysis of the combined effect of steel support diameter and wall thickness indicate that the two have a coupling effect on the safety of the pit; the diameter of the steel support can be reduced and

the wall thickness can be increased to achieve the same stabilising effect in special working conditions with space limitations.

(4) Compared with a 60% preloaded axial force level, 120% preloaded axial force can reduce the horizontal displacement of the pile top in the pit by about 10 mm and that of the surface settlement by about 4.2 mm. This finding indicates that the change in the preloaded axial force of the steel support affects the horizontal displacement of the enclosure structure and the surface settlement.

(5) From the perspective of pit safety, the pit can be concluded to be in a safe state when the preloaded axial force level is 60%. Thus, reducing the preloaded axial force level scientifically and reasonably is feasible under the premise of guaranteeing the safety of the pit in the actual construction process.

Author Contributions: Conceptualization, Y.J.; methodology, Y.J.; software, H.Z.; validation, C.Z. and C.D.; formal analysis, Y.J.; investigation, H.Z. and J.L.; resources, Y.J.; data curation, Y.J.; writing—original draft preparation, H.Z.; writing—review and editing, C.Z.; visualization, J.L. and C.D.; supervision, C.Z.; project administration, C.D.; funding acquisition, J.L. All authors have read and agreed to the published version of the manuscript.

Funding: This research was funded by the National Key Research and Development Program, grant numbers 2021YFB2600604 and 2021YFB2600600, and the patron is Zheng, C. Zheng Chuanfeng, male, 43 years old, Ph.D., School of Transportation, Jilin University, and The China Construction Group Seventh Engineering Bureau Research Project, grant number JTZB-CCDT-D005/2022, and the patron is Jin, Y. Yang Jin, male, 36 years old, China Construction 7th Bureau Transportation Construction Company Limited, senior engineer.

Data Availability Statement: Dataset available on request from the authors. The raw data supporting the conclusions of this article will be made available by the authors on request.

Conflicts of Interest: Authors Yang Jin, Jian Liu and Chong Ding were employed by the company China Construction 7th Bureau Transportation Construction Company Limited. The remaining authors declare that the research was conducted in the absence of any commercial or financial relationships that could be construed as a potential conflict of interest.

References

1. Sheng, Z.; Xuan, T.K.; Jiao, Y.S.; Bing, S. Fuzzy Reliability Analysis of Resistant Heave Stability for SMW-Protected Structure Deep Foundation Pit. In *Safety Science and Technology*; Li, S.C., Wang, Y.J., An, Y., Sun, X.Y., Li, X., Eds.; Science Press: Beijing, China, 2008; Volume 7, pp. 2144–2148.
2. Jin, Y.; Di, H.; Zhou, S.; Liu, H.; Wu, D.; Guo, H. Effects of Active Axial Force Adjustment of Struts on Support System during Pit Excavation: Experimental Study. *J. Geotech. Geoenviron. Eng.* **2024**, *150*, 04024027. [CrossRef]
3. Xie, Z.; Liu, X.; Niu, X.; Jian, J.; Xu, C.; Liao, J. Study on the Influence of the Performance Weakening of the Disconnectable Coupling (DC) Joint of Steel Support on the Retaining of a Foundation Pit. *Buildings* **2024**, *14*, 1330. [CrossRef]
4. Di, H.; Guo, H.; Zhou, S.; Chen, J.; Wen, L. Investigation of the Axial Force Compensation and Deformation Control of Servo Steel Struts in a Deep Foundation Pit Excavation in Soft. *Adv. Civ. Eng.* **2019**, *2019*, 5476354. [CrossRef]
5. Haque, M.E. An ANN Model for Biaxial Bending of Reinforced Concrete Column. In *System-Based Vision for Strategic and Creative Design*; Bontempi, F., Ed.; AA Balkema Publishers: Rotterdam, The Netherlands, 2003; pp. 1517–1521.
6. Muhtar. The Prediction of Stiffness Reduction Non-Linear Phase in Bamboo Concrete Beam Using the Finite Element Method (FEM) and Artificial Neural Networks (ANNs). *Forests* **2020**, *11*, 1313. [CrossRef]
7. Wang, Z.; Wang, C. Analysis of Deep Foundation Pit Construction Monitoring in a Metro in Jinan City. *Geotech. Geol. Eng.* **2019**, *37*, 813–822. [CrossRef]
8. Zhou, Z.; Sun, X.; Heng, C. Temperature Influence to the Steel Brace in Piles in Row-Steel Bracing. In Proceedings of the Advances in Underground Space Development, Singapore, 7–9 November 2012; Zhou, Y., Cai, J., Sterling, R., Eds.; Research Publishing Services: Singapore, 2013; pp. 1257–1264.
9. He, M.D.; Zhang, D.L.; He, M.D.; Liu, J.; Le, G.P. Analysis of Supporting Structure Deformation and Axial Force in Subway Pit. In *Rock Mechanics: Achievements and Ambitions*; Cai, M., Ed.; CRC Press: Boca Raton, FL, USA, 2012; pp. 629–634.
10. Kozlowski, M. Experimental and Numerical Assessment of Structural Behaviour of Glass Subjected to Soft Body Impact. *Compos. Struct.* **2019**, *229*, 111380. [CrossRef]
11. Wang, Z.; Guo, B.; Wei, G.; Hu, C.; Zhang, L. Simplified Deformation Analyses of a Single Pile Subjected to Different Modes of the Pit Enclosure Structure. *Int. J. Geomech.* **2023**, *23*, 04023014. [CrossRef]

12. Wang, Z.; Guo, B.; Wei, G.; Yao, D.; Hu, C. Study for Longitudinal Deformation of Shield Tunnel in Side of Foundation Pit Based on Virtual Image Technique. *Appl. Sci.* **2022**, *12*, 8745. [CrossRef]
13. Xu, Y.; Zhao, Y.; Jiang, Q.; Sun, J.; Tian, C.; Jiang, W. Machine-Learning-Based Deformation Prediction Method for Deep-Pit Enclosure Structure. *Appl. Sci.* **2024**, *14*, 1273. [CrossRef]
14. Isleem, H.F.; Chukka, N.D.K.R.; Bahrami, A.; Oyebisi, S.; Kumar, R.; Qiong, T. Nonlinear Finite Element and Analytical Modelling of Reinforced Concrete Filled Steel Tube Columns under Axial Compression Loading. *Results Eng.* **2023**, *19*, 101341. [CrossRef]
15. Luo, Y.; Chen, J.; Wang, H.; Sun, P. Deformation Rule and Mechanical Characteristics of Temporary Support in Soil Tunnel Constructed by Sequential Excavation Method. *Ksce J. Civ. Eng.* **2017**, *21*, 2439–2449. [CrossRef]
16. Pirmoz, A.; Danesh, F.; Farajkhah, V. The Effect of Axial Beam Force on Moment-Rotation Curve of Top and Seat Connections. *Struct. Des. Tall Spec. Build.* **2011**, *20*, 767–783. [CrossRef]
17. Hsu, C.-F.; Tsai, Y.-H.; Chen, Y.-R.; Li, Y.-F.; Chen, S.-L. Normalized Analysis of Deformation for Deep Excavation Diaphragm Walls under Different Neighboring Building Conditions. *Results Eng.* **2024**, *22*, 102155. [CrossRef]
18. Liu, J.; Yang, L.; Zhang, J.; Zhang, W. Stress Resultant Analysis of Steel Penstocks Using A Flat Shell Element. In *Progress in Civil Engineering*; Chu, M.J., Li, X.G., Lu, J.Z., Hou, X.M., Wang, X., Eds.; Elsevier: Amsterdam, The Netherlands, 2012; Volume 170–173, pp. 1887–1892.
19. Han, S.; Yang, K.; Wei, X.; Yun, L.; Cheng, C. Analysis of the Influence of inside and Outside Water Level Changes of foundation Pit on Stability of Foundation. In Proceedings of the 2nd International Conference on Architectural, Civil and Hydraulics Engineering (ICACHE 2016), Kunming, China, 29–30 September 2016; pp. 280–284.
20. Zhang, Y.; Wang, Y.; Zhao, Y. A Case Study on the Deformation of Metro Foundation Pit in Silt Stratum in North China. *Shock. Vib.* **2021**, *2021*. [CrossRef]
21. Cheng, X.; He, J.; Li, X.; Xia, Q.; Su, H.; Chen, C. Deformation rule of bored pile & steel support for deep foundation pit in sandy pebble geology. *Civ. Eng. J.-Staveb. Obz.* **2023**, *33*, 282–297. [CrossRef]
22. Wang, Q.; Ma, P.; Shi, Z. Study on Influence of Vertical Position of Steel Bracing in Foundation of Open Cut Railway on Deformation of Envelope Structure. *IOP Conf. Ser. Earth Environ. Sci.* **2020**, *455*, 012128. [CrossRef]
23. James, A.; Kurian, B. Diaphragm Wall Retaining System—A Simplified Model for Design Loads. *Aust. J. Civ. Eng.* **2022**, *20*, 374–388. [CrossRef]
24. Hua, J.; Zheng, J. *Geological Engineering Handbook*; China Architecture & Building Press: Beijing, China, 2018.
25. *DB22-T5020-2019*; Technical Standard for Monitoring Measurementof Urban Rail Transit ENGINEERING. Jilin Provincial Department of Housing and Urban-Rural Development: Changchun, China, 2019.